Biochemical Journal (2017) **474** 1619–1631
DOI: 10.1042/BCJ20170085

PORTLAND PRESS

Research Article

Staphylococcus aureus SdrE captures complement factor H's C-terminus via a novel 'close, dock, lock and latch' mechanism for complement evasion

Yingjie Zhang[1,*], Minhao Wu[2,3,*], Tianrong Hang[2,3,*], Chengliang Wang[2,3], Ye Yang[1], Weimin Pan[1], Jianye Zang[2,3], Min Zhang[1] and Xuan Zhang[2,3]

[1]School of Life Science, Anhui University, 111 Jiulong Road, Hefei 230601, China; [2]Hefei National Laboratory for Physical Sciences at Microscale, CAS Center for Excellence in Biomacromolecules, Collaborative Innovation Center of Chemistry for Life Sciences, and School of Life Sciences, University of Science and Technology of China, 96 Jinzhai Road, Hefei, Anhui 230026, China; and [3]Key Laboratory of Structural Biology, Chinese Academy of Sciences, 96 Jinzhai Road, Hefei, Anhui 230026, China

Correspondence: Xuan Zhang (xuanzbin@ustc.edu.cn) or Min Zhang (zhmin07@ustc.edu)

Complement factor H (CFH) is a soluble complement regulatory protein essential for the down-regulation of the alternative pathway on interaction with specific markers on the host cell surface. It recognizes the complement component 3b (C3b) and 3d (C3d) fragments in addition to self cell markers (i.e. glycosaminoglycans, sialic acid) to distinguish host cells that deserve protection from pathogens that should be eliminated. The *Staphylococcus aureus* surface protein serine–aspartate repeat protein E (SdrE) was previously reported to bind human CFH as an immune-evasion tactic. However, the molecular mechanism underlying SdrE–CFH-mediated immune evasion remains unknown. In the present study, we identified a novel region at CFH's C-terminus ($CFH^{1206–1226}$), which binds SdrE N2 and N3 domains ($SdrE_{N2N3}$) with high affinity, and determined the crystal structures of apo-$SdrE_{N2N3}$ and the $SdrE_{N2N3}$–$CFH^{1206–1226}$ complex. Comparison of the structure of the CFH–SdrE complex with other CFH structures reveals that CFH's C-terminal tail flips from the main body to insert into the ligand-binding groove of SdrE. In addition, $SdrE_{N2N3}$ adopts a 'close' state in the absence of CFH, which undergoes a large conformational change on CFH binding, suggesting a novel 'close, dock, lock and latch' (CDLL) mechanism for SdrE to recognize its ligand. Our findings imply that SdrE functions as a 'clamp' to capture CFH's C-terminal tail via a unique CDLL mechanism and sequesters CFH on the surface of *S. aureus* for complement evasion.

Introduction

As the first line of immune defence for humans, the complement system plays a crucial role in pathogen recognition, destruction and elimination [1]. This powerful defence system comprises more than 30 proteins in the blood or on the cell surface, which can be activated in a cascade-dependent process via three different pathways: the classic, lectin and alternative pathways [2,3]. The three pathways converge at the generation of complement component 3 (C3) and complement component 5 (C5) convertases, which results in cleavage of C3 into fragments C3a and C3b. The C3b fragment interacts with C5 convertase to cleave C5 into fragments C5a and C5b. On formation of the convertases, anaphylatoxins (C3a/C5a), the membrane-attack complex and opsonins (C3b) are generated [3–5].

The alternative pathway is crucial for amplification of the complement cascade, because it accounts for between 80% and 90% of total complement activation [6]. To avoid damage to host tissues, complement factor H (CFH) and C3b are applied to discriminate between host and foreign cells [5,7], with C3b spontaneously deposited on the surface of all cells (host cells, as well as pathogens) exposed to the activated complement system. CFH, a complement regulator in either soluble or membrane-

*These authors contributed equally to this work.

Received: 24 January 2017
Revised: 2 March 2017
Accepted: 3 March 2017

Accepted Manuscript online: 3 March 2017
Version of Record published: 4 May 2017

PORTLAND PRESS

Biochemical Journal (2017) 474 1619–1631
DOI: 10.1042/BCJ20170085

bound form, binds to the C3b and C3d fragments, as well as to host-cell markers [polyanions, such as glycosaminoglycans (GAGs) and sialic acid] to distinguish host cells from pathogens or altered host cells (e.g. cancer cells) and protect host cells from unintended complement-mediated injury.

CFH is composed of 20 complement-control protein (CCP) units (also known as short consensus repeats), with spacers consisting of three to eight amino acids between units. Each unit contains ∼60 amino acids, with the sequence highly conserved across units [8]. As a key regulator in the alternative pathway, CFH is abundant in serum, with a concentration of ∼500 mg/ml. However, fluctuations in serum CFH concentrations can range from 116 mg/ml to 562 mg/ml according to different environmental and genetic factors [9,10]. The important regulatory function and high concentration of CFH make it a favourable target for surface binding by pathogens, in order to disguise themselves as normal host cells and escape elimination by the complement system [11]. It has been reported that the surface-exposed lipoprotein fHbp of *Neisseria meningitidis* mimics the host carbohydrates to bind CFH–CCP6 [12]. The outer surface protein E (OspE) of *Borrelia burgdorferi* binds to CFH–CCP20 in a similar way to host cells binding CFH–CCP20 via GAGs [13]. In addition, *Staphylococcus aureus* surface protein SdrE, which belongs to the serine–aspartate repeat-containing protein (Sdr) subfamily within the microbial surface component recognizing adhesive matrix molecule (MSCRAMM) family, was recently reported to bind CFH as an immune-evasion tactic [14]. Sdr subfamily members adopt a similar structural pattern, including an N-terminal signal peptide (S), a functional ligand-binding region (A), a B region, a Ser–Asp repeated R region, a C-terminal cell wall membrane-spanning region (W), a hydrophobic membrane region (M) and a cytoplasmic tail (C). The N2 and N3 domains in the A region form IgG-like folds that bind ligands [15]. Although the fibrinogen (Fg)-bound structures of the N2–N3 domains of other MSCRAMM proteins, including SdrG [16], branch-point-binding protein (Bbp) [17], clumping factor A (ClfA) [18] and B (ClfB) [19], have been reported, little is known about how the newly identified ligand CFH is recognized by MSCRAMM family proteins. Furthermore, the molecular basis for SdrE–CFH recognition and SdrE–CFH-mediated immune evasion still remains to be elucidated.

In the present study, we mapped the minimal binding region [amino acids 1206–1226 ($CFH^{1206-1226}$)] in CFH–CCP20 for interaction with $SdrE_{N2N3}$, and solved the structures of apo-$SdrE_{N2N3}$ (PDB code: 5WTA) and the $SdrE_{N2N3}$–$CFH^{1206-1226}$ complex (PDB: 5WTB). Structural analysis and comparison with other MSCRAMM proteins revealed a novel closed state of SdrE, wherein the ligand-binding groove formed by the N2 and N3 domains is occupied by $Loop^{A-B}$ in the absence of ligand. To capture CFH's C-terminal tail, $Loop^{A-B}$ of $SdrE_{N2N3}$ rotates ∼180° to facilitate CFH binding. This indicates that SdrE recognizes its ligands by using a unique 'close, dock, lock and latch' (CDLL) mechanism observed in the MSCRAMM protein family for the first time. Compared with the structures of CFH in complex with C3b, fHbp or OspE, a large conformational change of the C-terminal tail of CFH was observed on SdrE binding, demonstrating a novel recognition mechanism between CFH and its ligands. All these findings illustrate that SdrE binds to a unique region in CFH's C-terminal region with a high affinity for capturing CFH for complement evasion. Our findings suggest that SdrE functions as a 'clamp' to capture the CFH C-terminal tail via a novel 'CDLL' mechanism and sequesters CFH on the surface of *S. aureus* to evade the human immune system.

Experimental

Cloning, expression and purification

DNA fragments encoding residues 270–599 of wild-type SdrE or its mutants were obtained by PCR and ligated to pET-22b(+) (Novagen) vector with a C-terminal 6×His tag. The construct was transformed into *Escherichia coli* BL21 (DE3) strain and grown with shaking overnight at 37°C in a 20-ml starter culture of Luria–Bertani (LB) medium containing 100 μg/ml of ampicillin. The overnight starter culture was then transferred into 1 l of LB medium and incubated at 37°C with shaking until reaching an absorbance at 600 nm of ∼0.6. The culture was then induced with 0.4 mM IPTG and incubated at 16°C for 18–24 h. The cells were harvested by centrifugation (277 K, 6000***g***, 8 min) and suspended in lysis buffer [50 mM Tris-HCl, pH 7.8, 500 mM NaCl and 5% (v/v) glycerol]. The cells were then homogenized by sonication and the lysate was centrifuged for 30 min at 12 000***g*** and 277 K. The supernatant was loaded onto a Ni/NTA nickel-chelating column (Qiagen) pre-equilibrated with lysis buffer. The column was washed by approximately 20 column volumes of lysis buffer with 40 mM imidazole to remove contaminants. The eluted target protein was concentrated by centrifugal ultrafiltration (Millipore, 10-kDa cut-off) and further purified using a Superdex 75 16/60 size exclusion column (GE Healthcare) equilibrated with buffer consisting of 20 mM Tris-HCl, pH 7.8, 400 mM NaCl, 5% (v/v) glycerol

Biochemical Journal (2017) **474** 1619–1631
DOI: 10.1042/BCJ20170085

and 1 mM DTT. Various truncated fragments and mutants of human CFH were amplified by PCR and cloned to the pGEX-6P-1 vector. The recombinant proteins were expressed in *E. coli* BL21 (DE3) strain and purified by GST affinity chromatography.

Crystallization and data collection

The apo-$SdrE_{N2N3}$ protein was concentrated to 20 mg/ml in 20 mM Tris-HCl, pH 7.8, 400 mM NaCl, 5% (v/v) glycerol and 1 mM DTT. The synthesized $CFH^{1206–1226}$ peptide and $SdrE_{N2N3}$ were mixed at a molar ratio of 5:1 and incubated at 277 K overnight. Initial crystallization screening was carried out at 298 K using a sitting-drop, vapour-diffusion method with commercial screen kits from Hampton Research (Crystal Screen, Crystal Screen 2, SaltRx 1, SaltRx 2, PEGRx 1, PEGRx 2 and Index). The apo-$SdrE_{N2N3}$ crystals were grown in 0.1 M citric acid, pH 3.5, 16% (w/v) PEG-3350 and 2% (v/v) 2-methyl-2,4-pentanediol (MPD). The complex crystals were obtained from 0.1 M Hepes, pH 7.5, 0.2 M magnesium chloride and 30% (v/v) PEG-400. X-ray diffraction data for apo-$SdrE_{N2N3}$ and the $SdrE_{N2N3}$–$CFH^{1206–1226}$ complex were collected at 100 K at Shanghai Synchrotron Radiation Facility (SSRF) beamline BL17U1 and BL18U1, respectively. Diffraction data were indexed, integrated and scaled using the programs iMOSFLM [20], POINTLESS [21] and SCALA [21] in the CCP4i suite [22].

Structure determination, refinement and analysis

The crystal structure of apo-$SdrE_{N2N3}$ was determined by molecular replacement using Phaser [23] in the CCP4i suite with $SdrG_{N2N3}$ (PDB: 1R17) as the search model. After several runs of structure refinement using the programs REFMAC5 [24] and COOT [25], the final model was refined to 2.3 Å (1 Å = 0.1 nm) resolution with an R_{work} of 19.4% and an R_{free} of 25.2%. The $SdrE_{N2N3}$–$CFH^{1206–1226}$ complex structure was solved by molecular replacement using apo-$SdrE_{N2N3}$ as the search model. The final model was refined to 3.3 Å resolution with an R_{work} of 22.2% and an R_{free} of 28.1%. The quality of the final models was analysed using the program MolProbity [26]. Data collection and model refinement statistics are shown in Table 1.

GST pull-down assay

Various truncated fragments and mutants of human CFH were overexpressed in *E. coli* BL21 (DE3) cells. The cells were suspended in lysis buffer [50 mM Tris-HCl, pH 7.8, 400 mM NaCl, 5% (v/v) glycerol and 1 mM DTT] and then homogenized by sonication. After centrifugation of the lysates, the supernatant was incubated with 30 μl of GST beads (pre-equilibrated in lysis buffer) at 4°C for 1 h. The beads were washed with 1 ml of lysis buffer three times to remove the impurities. Then GST beads immobilized with GST–CFH were incubated with purified wild-type $SdrE_{N2N3}$ or its mutant at 4°C for 1 h. The beads were washed with 1 ml of lysis buffer five times to remove proteins that were non-specific binding. Beads were boiled with SDS/sample buffer and proteins retained on the GST beads were analysed using SDS/PAGE (Figure 1B–D and see Figure 3B and D).

Isothermal titration calorimetry

The interaction between $SdrE_{N2N3}$ protein and GST–$CFH^{1206–1226}$ was analysed using isothermal titration calorimetry (ITC) with a MicroCal iTC200 instrument (GE Healthcare) at 20°C in 50 mM Tris, pH 7.8, 400 mM NaCl and 0.5 mM tris(2-carboxyl)phosphine (TCEP). Experimental data were fitted to a single binding-site model and analysed using the ITC data analysis module of Origin 7.0 (MicroCal) provided by the manufacturer (Figure 1E).

Results and discussion

The C-terminal tail of CFH–CCP20 binds to $SdrE_{N2N3}$ with high affinity

The CCP19–20 region of CFH was reported to be capable of discriminating between host and complement-activating cells [27–31]. It is essential for binding the C3d part of C3b, and for the self cell markers such as GAGs and sialic acids. Some pathogen-secreted proteins, including the PspC [32] protein from *Streptococcus pneumoniae* and OspE [13] from *B. burgdorferi*, were also reported to recruit CFH through their interaction with the CCP19–20 units. SdrE is a newly identified CFH-binding protein that belongs to MSCRAMM family, which normally uses the extracellular domains N2 and N3 to bind ligands. Therefore, we hypothesized that $SdrE_{N2N3}$ recruits CFH via interactions with CFH–CCP19–20 (Figure 1A).

PORTLAND PRESS

Biochemical Journal (2017) **474** 1619–1631
DOI: 10.1042/BCJ20170085

Table 1. Data collection and structure refinement statistics

	Apo-SdrE$_{N2N3}$	SdrE$_{N2N3}$–CFH$^{1206–1226}$
Data collection		
Space group	*P*1	$P2_12_12_1$
PDB ID	5WTA	5WTB
Unit cell parameters		
a, b, c (Å)	41.81, 61.73, 139.61	117.50, 117.50, 154.39
α, β, γ (°)	80.89, 89.83, 73.34	90.00, 90.00, 90.00
Resolution range (Å)	40.01–2.30 (2.42–2.30)[1]	49.75–3.30 (3.48–3.30)
Wavelength (Å)	0.9792	0.9779
Unique reflections	55 992	31 291
Completeness (%)	95.5 (95.2)	96.1 (97.9)
Overall $I/\sigma(I)$	7.8 (3.4)	7.0 (1.9)
Multiplicity	2.2 (2.3)	2.8 (2.8)
R_{sym} (%)[2]	8.1 (26.4)	10.4 (56.1)
Refinement		
Resolution range (Å)	40.00–2.30	49.75–3.30
R_{work}[3]	0.194	0.222
R_{free}[4]	0.252	0.281
RMSD bond lengths (Å)	0.013	0.010
RMSD bond angles	1.408	1.371
Average B-factors (Å^2)		
Protein	22.2	89.5
Water	26.4	
Ramachandran plot[5]		
Most favoured regions (%)	97.1	90.4
Allowed regions (%)	2.9	9.6
Generously allowed regions (%)	0.0	0.0
MolProbity		
Clash score[6]/percentile	8.89/96	24.63/89
Overall score/percentile	2.20/81	3.31/80

[1]The values in parentheses refer to statistics in the highest shell.
[2]$R_{sym} = |I_i - \langle I \rangle| / \langle I \rangle$ where I_i is the intensity of the *i*th measurement, and $\langle I \rangle$ is the mean intensity for that reflection.
[3]$R_{work} = \Sigma_{hkl} ||F_{obs}| - k|F_{cal}|| / \Sigma_{hkl} |F_{obs}|$ where F_{obs} and F_{cal} are observed and calculated structure factors, respectively, calculated over all reflections used in the refinement.
[4]R_{free}, is similar to R_{work} but calculated over a subset of reflections (5%) excluded from all stages of refinement.
[5]Statistics for the Ramachandran plot from an analysis using MolProbity.
[6]The MolProbity clash score indicates the number of steric overlaps >0.4 Å per 1000 atoms.

To test our hypothesis, we constructed four CFH fragments (CFH$^{1107–1138}$, CFH$^{1139–1168}$, CFH$^{1166–1196}$ and CFH$^{1195–1231}$) within CCP19–20 fused to a GST tag at the N-terminus. *In vitro* GST pull-down assays confirm that the C-terminal 37 amino acids of CFH–CCP20 (CFH$^{1195–1231}$) are capable of interacting with SdrE$_{N2N3}$ (Figure 1B). To identify the shortest region in CFH–CCP20 responsible for SdrE$_{N2N3}$ binding, shorter CFH fragments were used for GST pull-down assays. As shown in Figure 1(C and D), a minimal segment containing 21 amino acid residues (CFH$^{1206–1226}$) is sufficient for SdrE$_{N2N3}$ interaction.

Kajander et al. [33] reported that the CCP19–20 region binds the C3d fragment primarily through the CCP20 site, but binds C3b through the CCP19 site, and proposed a comprehensive molecular mechanism for target discrimination mediated by CFH in the alternative pathway. On host-cell surfaces, CFH binds to the C3b

Biochemical Journal (2017) **474** 1619–1631
DOI: 10.1042/BCJ20170085

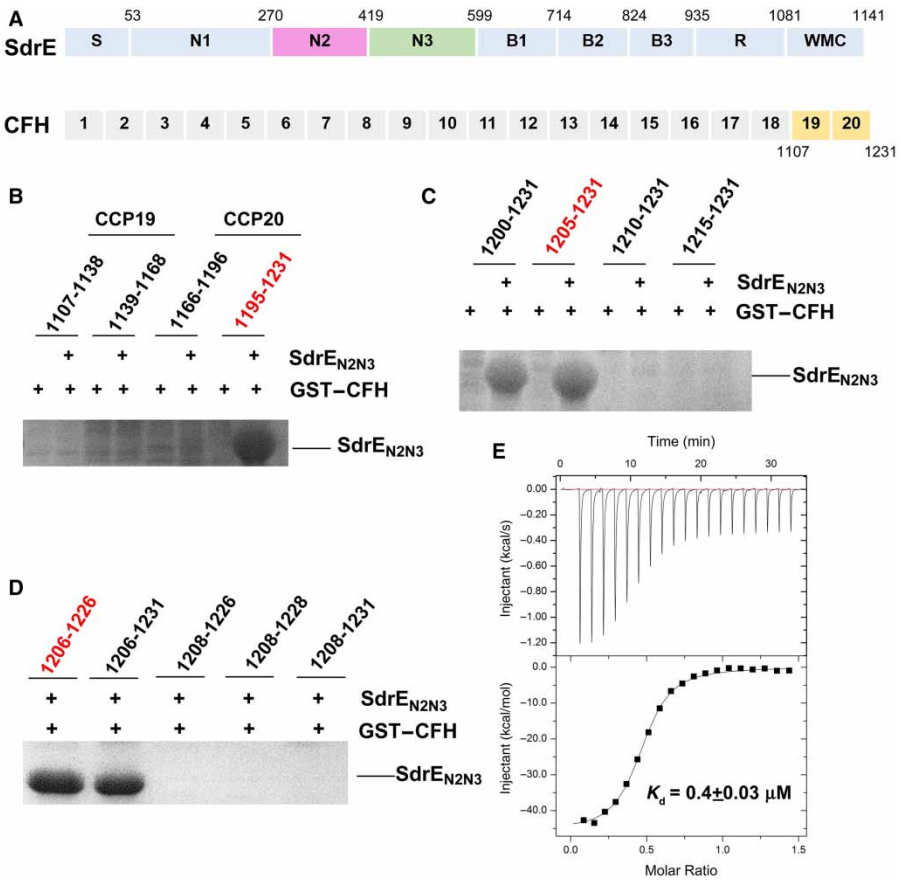

Figure 1. CFH–CCP20 is responsible for SdrE$_{N2N3}$ binding

(**A**) Schematic representation of SdrE and CFH domain organization. S, signal sequence; N1–N3, ligand-binding region; B1–B3, B repeats region; R, serine–aspartate repeat region; W, wall-spanning region; M, membrane-spanning region; C, cytoplasmic, positively charged tail. The amino acid residue number identifying the boundary between each subdomain is indicated above. (**B–D**) GST pull-down assays of SdrE$_{N2N3}$ with different fragments of the CFH fused to a GST tag. The retaining amino acid residues of each CFH fragment are indicated in each panel. (**E**) The ITC fitting curves of GST–CFH$^{1206–1226}$ to SdrE$_{N2N3}$.

site and cell surface markers through CCP19 and CCP20 sites, respectively. This causes the rapid down-regulation of the alternative pathway and converts C3b to C3d on host-cell surfaces, resulting in additional CFH proteins recruited to the surface. While localized on the surfaces of pathogens lacking host-cell markers, CCP19–20 binds to C3b with lower affinity, subsequently activating the alternative pathway and initiating pathogen elimination [33,34]. To evade complement-mediated destruction, some pathogens use surface proteins to sequester CFH to their cell surface. After confirming that the CFH–CCP20 domain is recognized by SdrE$_{N2N3}$, we determined the binding affinity of CCP20 to SdrE$_{N2N3}$, revealing that SdrE$_{N2N3}$ strongly interacts with CFH$^{1206–1226}$, with a dissociation constant (K_d) value of ~0.4 μM (Figure 1E), which is as high as that measured for the CCP20–C3d interaction [33]. These findings indicate that the relatively strong binding of SdrE to CCP20 promotes efficient recruitment of CFH to the cell surface of *S. aureus* for complement disguise.

A novel 'close' state of apo-SdrE$_{N2N3}$ with the ligand-binding groove occupied by Loop$^{A–B}$

To investigate the molecular basis for CFH recognition by SdrE, we solved the crystal structures of apo-SdrE$_{N2N3}$ and SdrE$_{N2N3}$ in complex with CFH$^{1206–1226}$. SdrE$_{N2N3}$ exists as a monomer in both solution and its crystal form (see Supplementary Figure S1). Four apo-SdrE$_{N2N3}$ monomers were found in one asymmetrical unit. Each subunit consists of two distinct domains: N2 (residues 270–419) and N3 (residues 420–586)

Biochemical Journal (2017) **474** 1619–1631
DOI: 10.1042/BCJ20170085

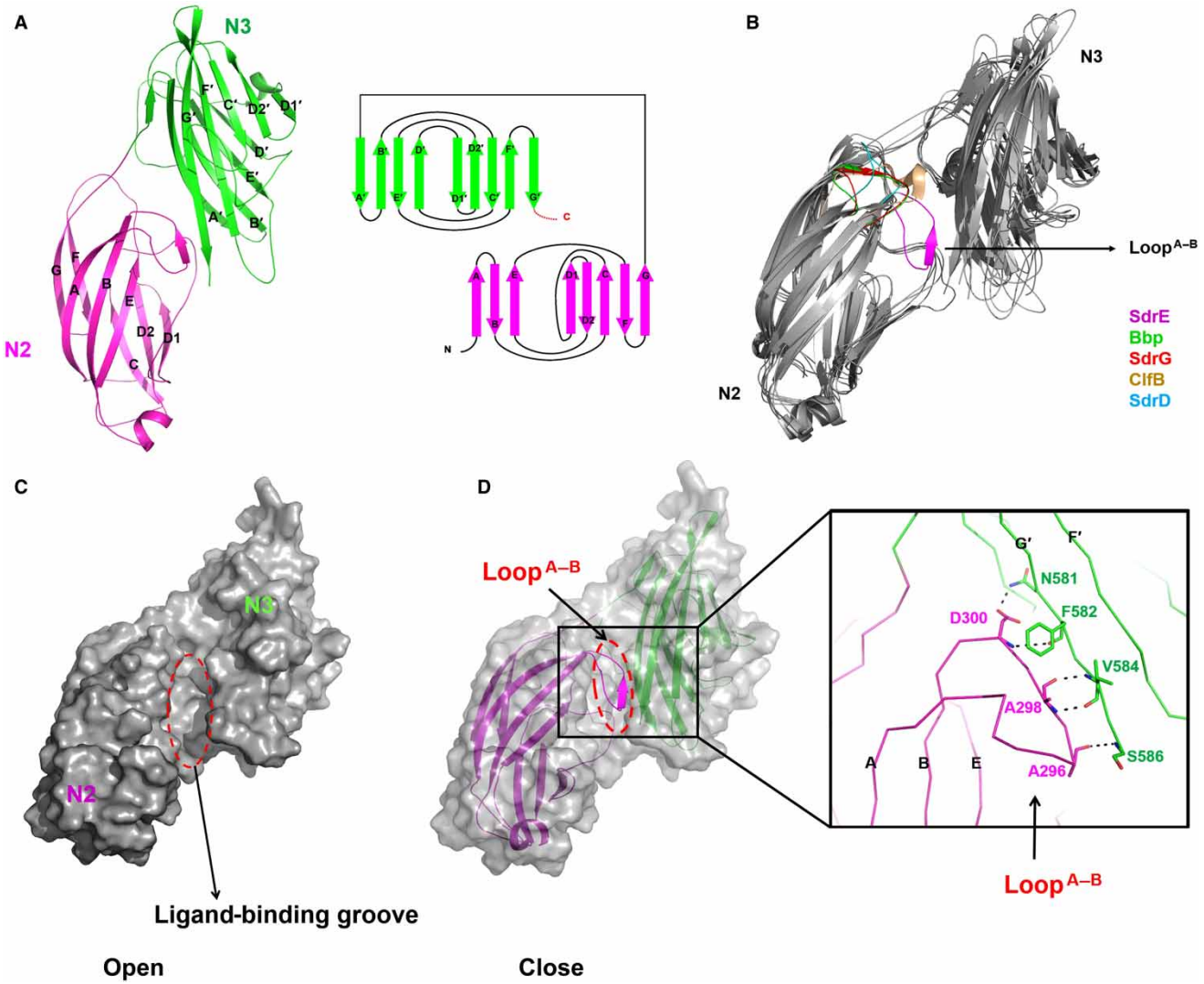

Figure 2. Crystal structure of apo-SdrE$_{N2N3}$

(**A**) Cartoon representation of the structure of apo-SdrE$_{N2N3}$ and a schematic representation of the topology of the SdrE$_{N2N3}$ fold. The N2 and N3 domains are shown in purple and green, respectively. (**B**) Structural comparison of apo-SdrE$_{N2N3}$ with its homologous structures; Loop$^{A–B}$ is coloured purple for SdrE, green for Bbp, red for SdrG, wheat for ClfB and blue for SdrD. (**C**) Surface representation of the 'open' state of apo-SdrE$_{N2N3}$ with the Loop$^{A–B}$ deleted from the structure. (**D**) Cartoon representation of the 'close' state of apo-SdrE$_{N2N3}$. The N2 and N3 domains are shown in purple and green, respectively. The ligand-binding groove is highlighted by a dashed red ellipse. Key residues that stabilize the 'close' state are shown as sticks.

(Figure 2A), packing against each other and separated by a short linker region. The N2 and N3 domains contain eight (A↑B↓C↑D1↑D2↓E↑F↓G↑) and nine (A′↓B′↑C′↓D′↑D1′↓D2′↑E′↓F′↑G′↓) antiparallel β-strands, respectively. The topologies of N2 and N3 domains are structurally similar, with both resembling the IgG-like fold, except that N2 lacks the D-strand (Figure 2A). Structural comparison with other reported MSCRAMM proteins reveals similar overall structures between SdrE$_{N2N3}$ and Bbp (PDB: 5CF3, RMSD of 2.7 Å over 304 Cα atoms), SdrG (PDB: 1R19, RMSD of 2.6 Å over 276 Cα atoms), ClfB (PDB: 4F24, RMSD of 3.4 Å over 237 Cα atoms) and SdrD (PDB: 4JE0, RMSD of 4.7 Å over 229 Cα atoms), but a novel 'close' state with the ligand-binding groove occupied by Loop$^{A–B}$ (Figure 2B). The Loop$^{A–B}$ in SdrE homologues either turns around to interact with the N2–N3 linker and G-strand in Bbp, SdrG and ClfB, or locates by the side of the groove as a loop in SdrD, to leave the groove in an 'open' state for ligand binding. However, the Loop$^{A–B}$ in SdrE extends

Biochemical Journal (2017) **474** 1619–1631
DOI: 10.1042/BCJ20170085

from the N2 domain to form a pair of antiparallel β-sheets with the G′-strand in the N3 domain. The β-sheet is stabilized by four pairs of main-chain hydrogen bonds, resulting in the ligand-binding groove of $SdrE_{N2N3}$ being locked in a 'close' state (Figure 2C and D).

It is not the first time that the 'close' conformation of MSCRAMM proteins has been mentioned. A 'dock, lock and latch' (DLL) model was proposed for the SdrG based on its apo- and Fg-peptide-bound structures [16]. In this model, the Fg peptide docks into the 'open'-form groove first. Then the C-terminal tail of N3 extends forward to 'lock' the peptide in place and an additional G″-strand is formed to 'latch' on to the peptide–SdrG complex by interacting with the N2 domain. A 'close' conformation of SdrG, which was generated by introducing a disulfide bond between the latch and the N2 domain, cannot bind Fg, demonstrating that the 'open' state of the ligand-binding groove of SdrG is required for the initial docking of the ligand [16]. However, a ClfA mutant, exhibiting an artificially closed binding groove through the introduction of a disulfide bond in a similar manner, retains the ability to bind Fg with lower affinity compared with that observed in wild-type proteins. Therefore, a different ligand-binding mechanism, the 'latch, dock' (LD) model, was proposed for ClfA [18]. Although this 'close' conformation was proposed, up until now no structural or other evidence was reported to clearly confirm this state of MSCRAMM proteins. The 'close' state observed in the SdrE structure, in contrast to the previously proposed 'close' state artificially formed by the 'latch' of the N3 domain, is formed by $Loop^{A–B}$ protruding into the N2 domain to occupy the ligand-binding groove. This novel 'close' state suggests a new ligand-binding mechanism for SdrE.

$CFH^{1206–1226}$ is recognized by $SdrE_{N2N3}$ via a CDLL mechanism

For further investigation, we solved the crystal structure of the $SdrE_{N2N3}$–$CFH^{1206–1226}$ complex. One $SdrE_{N2N3}$ molecule and one $CFH^{1206–1226}$ molecule form a heterodimer. Four $SdrE_{N2N3}$–$CFH^{1206–1226}$ heterodimers, named heterodimer A–D, are found in one asymmetrical unit (see Supplementary Figure S2). Two $SdrE_{N2N3}$–$CFH^{1206–1226}$ heterodimers form a tetramer via interaction of the C-terminal of four amino acids with the two CFH peptides (see Supplementary Figure S2). Gel filtration and PISA (proteins, interfaces, structures and assemblies) analysis clarify that the $SdrE_{N2N3}$–$CFH^{1206–1226}$ complex exists as a heterodimer in both solution and crystal form, respectively (see Supplementary Figure S2). Therefore, the tetrameric conformation associated with the $SdrE_{N2N3}$–$CFH^{1206–1226}$ structure was caused by crystal packing. The overall structures of the four $SdrE_{N2N3}$ molecules are almost identical, with an average RMSD of 0.3 Å over 330 aligned Cα atoms. To simplify the description, we discuss only heterodimer A. As shown in Figure 3A, the CFH peptide forms a long β-strand and threads the ligand-binding groove between the N2 and N3 subdomains. Apart from four C-terminal residues (1223–1226), a well-defined electron density map is observed for the main chain of all other residues (1206–1222) and the side chain of some residues (see Supplementary Figure S3). Similar to Fg-bound Bbp, SdrG, ClfB and ClfA structures [16–19] (see Supplementary Figure S4), the CFH peptide forms an antiparallel β-sheet with G′-strand in N3, whereas the C-terminal G′-strand undergoes a rotation to surround the N-terminus of the CFH peptide. The C-terminal residues (587–598) missing in the apo-$SdrE_{N2N3}$ structure are ordered as a G″-strand on CFH binding in the complex structure, and extend to the N2 domain to compose complete β-sheets together with strands A, B and E (Figure 3A). The buried surface between $SdrE_{N2N3}$ and CFH is considerably larger, approximately 1100 $Å^2$. A total of 13 pairs of antiparallel, main-chain hydrogen bonds are formed by $SdrE_{N2N3}$ and the CFH peptide (see Supplementary Figure S5). All residues in $SdrE_{N2N3}$ involved in the CFH binding belong to the G′-strand (572–586), demonstrating a critical role of the G′-strand in the $SdrE_{N2N3}$–CFH interaction. In addition, side-chain interactions between $SdrE_{N2N3}$ and CFH include four hydrogen bonds and one hydrophobic interaction. The carbonyl oxygen of Asp^{334} and Asp^{588} from $SdrE_{N2N3}$ form hydrogen bonds with Ser^{1208} and Arg^{1206} from CFH, respectively. The main-chain nitrogen of $SdrE^{F433}_{N2N3}$ forms the hydrogen bond with the side-chain oxygen of CFH^{S1209}. The side-chain nitrogen of $SdrE^{Q419}_{N2N3}$ contributes another hydrogen bond via interaction with the hydroxyl group of CFH^{S1211}. A hydrophobic pocket created by Leu^{335}, Leu^{436} and Ile^{583} from $SdrE_{N2N3}$ mediates the hydrophobic interaction with the side chain of CFH^{L1207} (Figure 3A).

To verify our complex structure, $SdrE_{N2N3}$ residues Asp^{334}, $Leu3^{35}$, Gln^{419} and Asp^{588}, which interact with CFH through side chains, were mutated to alanine, and their interaction with $CFH^{1206–1226}$ was evaluated by GST pull-down assays. As shown in Figure 3B, the mutations D334A, L335A and Q419A significantly weaken the interaction between $SdrE_{N2N3}$ and CFH, whereas the mutation D588A absolutely abolishes the interaction. Consistent with the structural analysis, our mutagenesis studies confirm the important roles of Asp^{334}, Leu^{335}, Gln^{419} and Asp^{588} from SdrE in the $SdrE_{N2N3}$–CFH interaction. To identify residues of $CFH^{1206–1226}$ that are

Biochemical Journal (2017) **474** 1619–1631
DOI: 10.1042/BCJ20170085

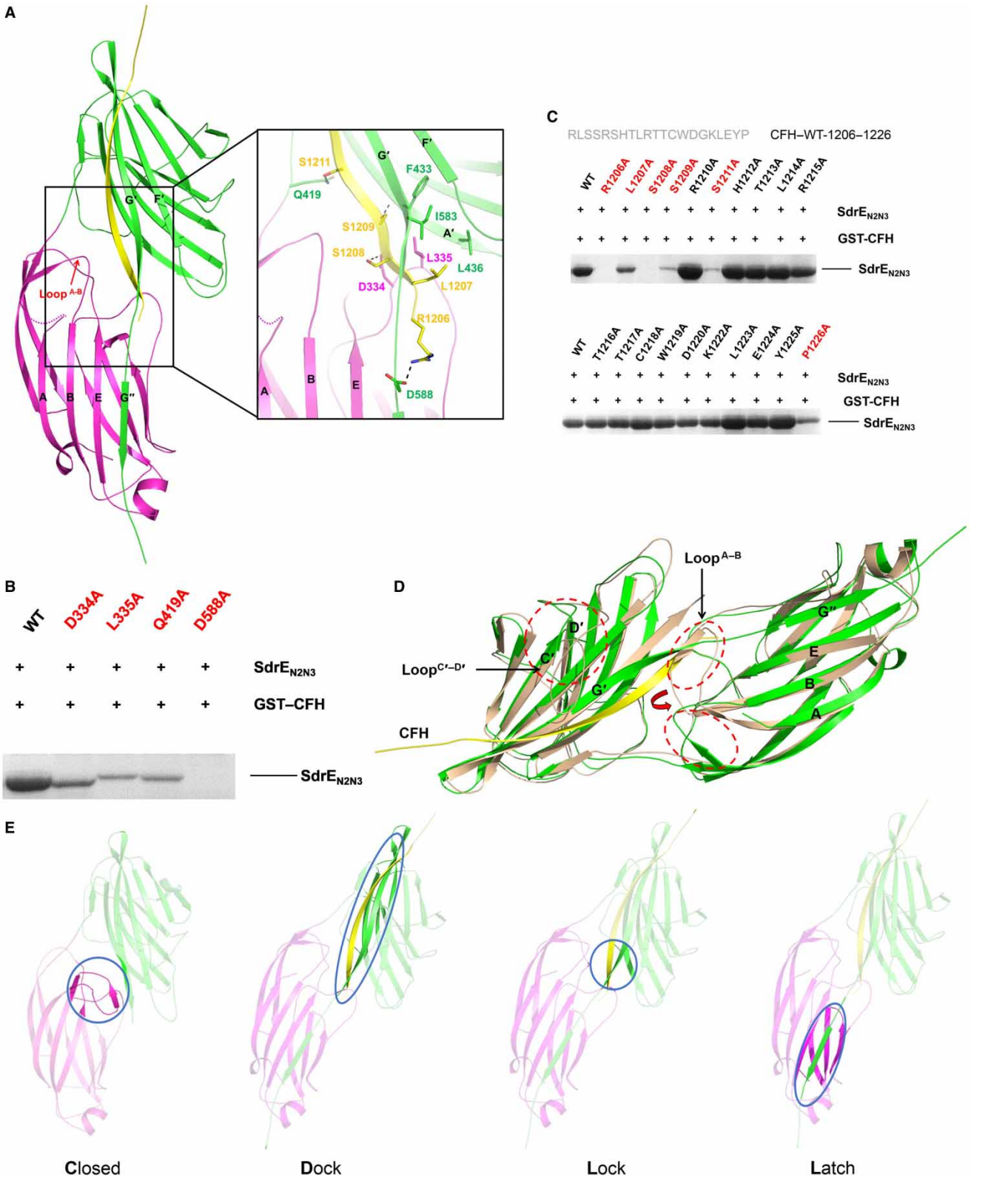

Figure 3. Crystal structure of the $SdrE_{N2N3}$–$CFH^{1206–1226}$ complex Part 1 of 2

(**A**) Cartoon representation of the $SdrE_{N2N3}$–$CFH^{1206–1226}$ complex. N2 and N3 subdomains from the SdrE and the CFH peptide are coloured purple, green and yellow, respectively. $Loop^{A–B}$ is indicated by a red arrow. Key residues involved in the side-chain interactions between SdrE and CFH are

Biochemical Journal (2017) **474** 1619–1631
DOI: 10.1042/BCJ20170085

Figure 3. Crystal structure of the $SdrE_{N2N3}$–$CFH^{1206–1226}$ complex Part 2 of 2

shown as sticks in the zoom-in view. Hydrogen bonds involved in the SdrE–CFH interaction are shown as black dashes. (**B**) GST pull-down assays of GST–$CFH^{1206–1226}$ with $SdrE_{N2N3}$ and its mutants. (**C**) Identification of the key residues on CFH–CCP20 for SdrE binding. Key residues are coloured red. (**D**) Structural comparison of apo-$SdrE_{N2N3}$ (wheat) and the $SdrE_{N2N3}$–$CFH^{1206–1226}$ complex (green). $Loop^{A–B}$ and $Loop^{C'–D'}$ are circled by red dashes and labelled in black. The change of the two conformations of $Loop^{A–B}$ is indicated by a red arrow. (**E**) A CDLL model for the SdrE–CFH interaction is shown as a cartoon.

important for binding $SdrE_{N2N3}$, each residue within $CFH^{1206–1226}$ (except for alanine and glycine) was sequentially substituted by alanine (Figure 3C). The binding ability of each mutant for $SdrE_{N2N3}$ was tested *in vitro* by GST pull-down assays. Remarkably, the mutations R1206A and S1208A absolutely abolish the interaction of CFH with $SdrE_{N2N3}$. Interaction between CFH and $SdrE_{N2N3}$ is significantly weakened by the mutations S1209A and S1211A, whereas mutation L1207A results in the loss of half the binding capacity of CFH with $SdrE_{N2N3}$. Therefore, Arg^{1206}, Leu^{1207}, $Ser1^{208}$, Ser^{1209} and Ser^{1211} are the key residues of CFH for $SdrE_{N2N3}$ binding.

To investigate the ligand-binding mechanism associated with the $SdrE_{N2N3}$–CFH interaction, we compared the apo-$SdrE_{N2N3}$ structure with that of the $CFH^{1206–1226}$-bound form. The overall structure of $SdrE_{N2N3}$ in either apo- or $CFH^{1206–1226}$-bound form is similar, with an RMSD of 2.8 Å over 293 aligned Cα atoms. Several significant conformational changes caused by the interaction of the CFH peptide are observed (Figure 3D). First, $Loop^{A–B}$ rotates ∼180° away from the ligand-binding groove to interact with the N2–N3 linker and the G-strand, which converts the 'close' groove to the 'open' conformation for CFH binding. Second, residues from Val^{468} to Leu^{476} from $Loop^{C'–D'}$ become disordered after the 'dock' procedure with the CFH peptide. This region of $Loop^{C'–D'}$ localizes in close proximity to the CFH-binding site in the apo-$SdrE_{N2N3}$ structure; however, after CFH binding, this region could be dislocated and become disordered. The third and most significant difference is the formation of the 'lock' and 'latch' structures in the $SdrE_{N2N3}$–CFH complex. The C-terminus of the G′-strand bends around the N-terminal region of the CFH peptide to 'lock' the ligand in place, and extends further to form an additional G″-strand to create β-sheets with β-strands in the N2 domain, thereby functioning as a 'latch'. The novel 'close' state of apo-$SdrE_{N2N3}$ and the structural comparison of apo-$SdrE_{N2N3}$ and $CFH^{1206–1226}$-bound $SdrE_{N2N3}$ indicate a novel ligand-binding mechanism as a 'CDLL' model among MSCRAMM proteins (Figure 3E). In addition, the 'close' conformation implicates potential regulatory mechanisms associated with SdrE by unknown cellular components.

SdrE functions as a 'clamp' to capture the C-terminal tail of the CFH for complement evasion

CFH functions as a host-recognition molecule and complement regulator in the alternative pathway. Normal recognition of host cells by the CFH requires the interaction of different CFH–CCP complexes with C3b and markers on the cell surfaces. CCP1–4 and CCP19–20 represent binding sites for C3b [4,35]. The crystal structure of the CCP19–20–C3d complex revealed that C3d binds to both CCP19 and -20 [33] (Figure 4A). CCP6 and CCP20 are capable of binding heparin and other polyanions, including GAGs [36,37], and CCP20 was also reported to be a sialic acid-binding site [38] (Figure 4B). Among all 20 CCP units, the C3b and host cell marker-binding sites on CCP19–20 play key roles in host recognition/discrimination and complement regulation. The dual interaction of CFH with C3b via the CCP19 site and with cell surface polyanions (heparin, GAGs, sialic acid) via the CCP20 site ensures optimal binding between the CFH and the host-cell surface. This results in rapid down-regulation of the alternative pathway and recruitment of additional CFH proteins to the surface to protect host cells. In contrast, microbes that lack such polyanions have far fewer CFH proteins located on their surfaces and are thereby susceptible to subsequent complement-mediated destruction. To escape elimination by the alternative pathway, some pathogens have developed novel strategies to recruit CFH to their surfaces, thus disguising themselves as normal host cells and evading immune attack. *N. meningitidis* subverts immune responses by using the surface protein fHbp to mimic host carbohydrates to recruit CFH [12]. Structural analysis combined with biochemical studies demonstrates that fHbp interacts with CFH–CCP6.

Biochemical Journal (2017) **474** 1619–1631
DOI: 10.1042/BCJ20170085

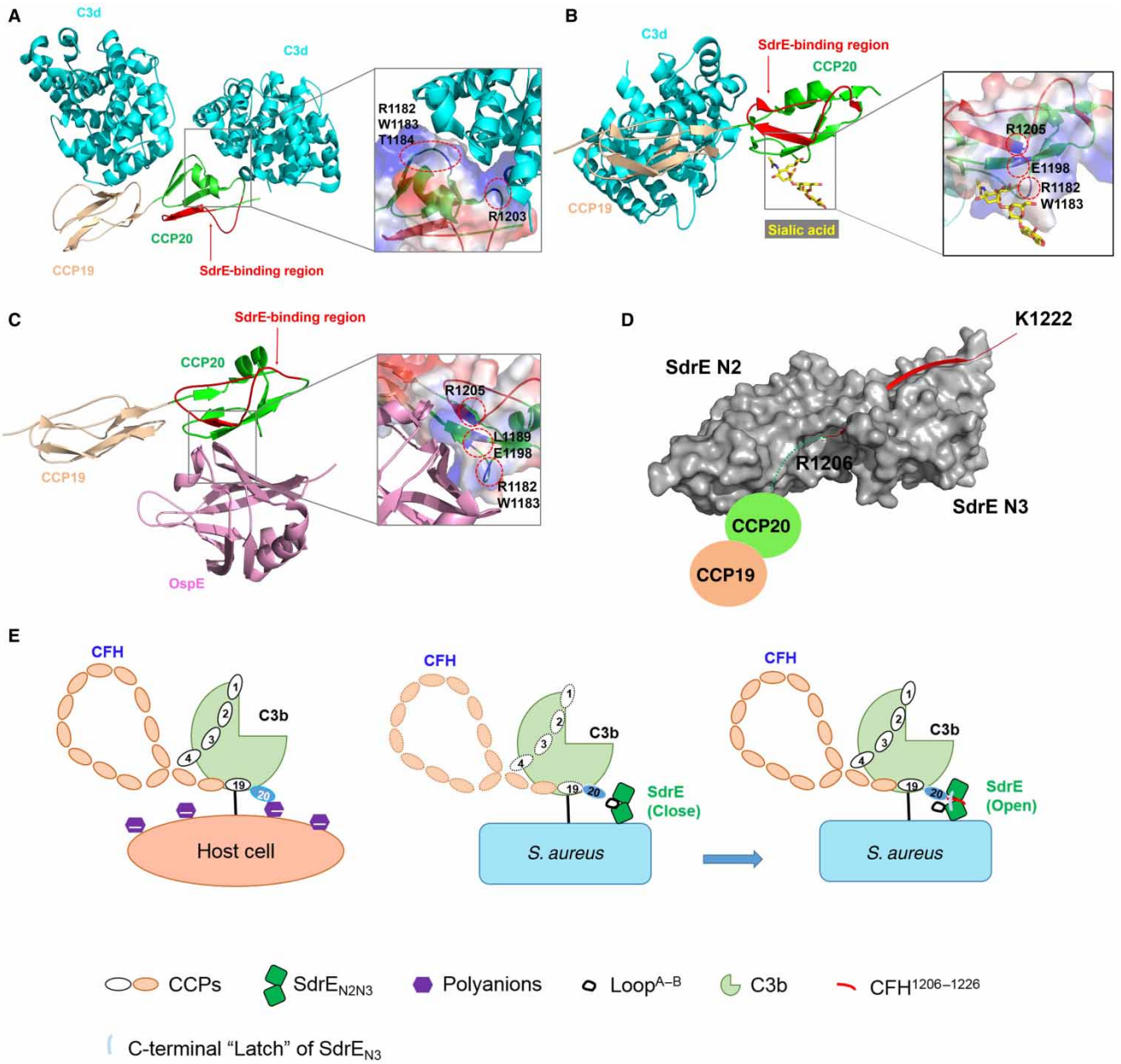

Figure 4. Structural comparison of the SdrE$_{N2N3}$–CFH$^{1206–1226}$ complex with C3d/sialic acid/OspE–CFH complexes

(**A**–**D**) Cartoon representation of crystal structures of CFH–CCP19–20 complexed with (**A**) C3d (cyan), (**B**) sialic acid (yellow), (**C**) OspE (pink) and (**D**) SdrE$_{N2N3}$ (grey). CCP19 and CCP20 are coloured wheat and green, respectively. The SdrE-binding region on CCP20 is coloured and labelled red. Binding sites on CCP20 for C3d, sialic acid and OspE are shown in zoom-in windows, with the key residues on CCP20 labelled in black and highlighted by dashed red circles. (**E**) Proposed model for the CFH–SdrE-mediated immune evasion mechanism.

The interaction interface between fHbp and CFH–CCP6 overlaps with the GAG-binding site on CFH–CCP6. Another outer surface protein, OspE of *B. burgdorferi,* was recently reported to bind to the same site as GAGs and sialic acid in CFH–CCP20 (Figure 4B and C) [13]. However, the binding site for SdrE on the CFH is unique (Figure 4D). In the present study, we identified Arg^{1206}, Leu^{1207}, Ser^{1208}, Ser^{1209} and Ser^{1211} of the CFH as the key residues required for SdrE$_{N2N3}$ binding (see Figure 3C). These differ from the residues in CFH–CCP20 identified for C3d binding (1182, 1183, 1184 and 1203) [33], binding of the cell markers heparin, GAGs and sialic acid (1182, 1183, 1186, 1188, 1189, 1198, 1215 and 1230) [38,39], and binding to the pathogen

surface protein OspE (1182, 1183, 1189, 1198 and 1215) (Figure 4A–D) [13]. Although SdrE recruits CFH by interacting with CCP20, which represents a common binding site for surface proteins from different pathogens, our structural and biochemical analysis demonstrated that the interaction region in CCP20 and the CFH-binding mechanism associated with SdrE were unique (Figure 4A–D).

Structural comparison of CFH peptide bound to $SdrE_{N2N3}$ with CFH–CCP20 complexed with C3d, sialic acid or OspE reveals a big conformational change of the C-terminal tail of CCP20 on SdrE binding (Figure 4A–D). CCP20 interacts with C3d and sialic acid mainly through electrostatic interactions, mediated by its positively charged surface regions. The *B. burgdorferi* surface protein OspE also uses a similar mechanism to bind the same region on CCP20 where sialic acid binds. Unique among these CFH ligands, SdrE's structural features make it suitable to function as a 'clamp' for capturing CFH's C-terminal tail. As shown in the model in Figure 4(E), SdrE adopts a 'close' conformation after integration on to the *S. aureus* surface during infection. When the host complement component C3b is deposited on the *S. aureus* surface, CFH binds to C3b through CCP1–4 and CCP19. Simultaneously, $Loop^{A–B}$ of $SdrE_{N2}$ rotates ∼180° to convert the 'close' conformation to an 'open' one to accommodate the C-terminal tail of CFH–CCP20. By undergoing a big conformational change, CCP20's C-terminal tail protrudes from the CFH to dock into the ligand-binding groove of $SdrE_{N2N3}$ by forming an antiparallel β-sheet with the G′-strand of $SdrE_{N3}$. In addition, $SdrE_{N2N3}$ functions as a 'clamp' to strongly stabilize the CFH–SdrE complex by locking and latching the CFH tail in its ligand-binding groove (see Figures 3 and 4C). Given that SdrE binds to CFH with a high affinity and functions as a 'clamp' to capture CFH's C-terminal tail, SdrE efficiently recruits CFH proteins to *S. aureus* surfaces, followed by *S. aureus* recruitment of factor I using CFH–CCP1–4 and its surface protein ClfA to cleave C3b into iC3b [40]. In addition, to decrease C3b deposition, CFH also accelerates the decay of already formed C3 convertase C3bBb [41], thereby limiting the amplification of the complement pathway. By using an SdrE–CFH-mediated immune evasion strategy, *S. aureus* is capable of successfully disguising itself as a host cell to evade host complement attack.

Conclusion

Many pathogens have developed immune-evasion strategies by recruiting CFH to their surfaces to disguise themselves as normal host cells, thus escaping elimination by the complement pathway. In the present study, we identified the minimal fragment of CFH responsible for interaction with the *S. aureus* surface protein SdrE and determined the crystal structures of apo-$SdrE_{N2N3}$ and the $SdrE_{N2N3}$–$CFH^{1206–1226}$ complex. Structural analysis and biochemical studies demonstrate that SdrE binds to a unique region of CFH–CCP20 relative to the binding sites on CCP20 for other CFH ligands, including host-cell markers and pathogenic virulence factors. In contrast to reported molecular mechanisms associated with CFH-mediated immune evasion, SdrE recognizes CFH–CCP20 with a CDLL mechanism and functions as a 'clamp' to capture CFH's C-terminal tail for complement evasion. Our results not only provide insights into the molecular mechanism of *S. aureus*'s complement disguise, but also shed light on the development of new therapeutics for the increasingly serious infections of *S. aureus*.

Abbreviations

C3, complement component 3; C5, complement component 5; CCP, complement-control protein; CFH, complement factor H; Fg, fibrinogen; GAG, glycosaminoglycan; ITC, isothermal titration calorimetry; LB, Luria–Bertani; MSCRAMM, microbial surface component recognizing adhesive matrix molecule; OspE, outer surface protein E; SdrE, serine–aspartate repeat protein.

Author Contribution

J. Zang, X. Zhang and M. Zhang provided the scientific direction and overall experimental design for the studies, Y. Zhang and T. Hang designed and performed the biochemical experiments, M. Wu was responsible for the crystal structure studies, and M. Wu and X. Zhang wrote the manuscript.

Funding

This work was supported by the Strategic Priority Research Program of the Chinese Academy of Sciences [Grant No. XDB 08010101], the National Key Research and Development Program of China [Grant no. 2016YFA0400903] and the Foundation for Innovative Research Groups of the National Natural Science Foundation of China [Grant no. 31621002]. This work was also supported by the National Natural Science

Biochemical Journal (2017) **474** 1619–1631
DOI: 10.1042/BCJ20170085

Foundation of China [Grant Nos. U1532109, 31370756 and 31361163002], and the Scientific Research Grant of Hefei Science Centre of CAS [Grant Nos. 2015SRG-HSC043 and 2015HSC-UP019] to J. Zhang. This work was also supported by the Anhui Provincial Natural Science Foundation [Grant no. 1608085QC52] for X. Zhang and the National Natural Science Foundation of China [Grant no. 31400627] for M. Wu.

Acknowledgements

We thank the staff at beamline BL17U1 and BL18U1 of the Shanghai Synchrotron Radiation Facility for assistance with data collection.

Competing Interests

The Authors declare that there are no competing interests associated with the manuscript.

References

1 Janeway, Jr, C.A. and Medzhitov, R. (2002) Innate immune recognition. *Annu. Rev. Immunol.* **20**, 197–216 doi:10.1146/annurev.immunol.20.083001.084359
2 Zipfel, P.F. (2009) Complement and immune defense: from innate immunity to human diseases. *Immunol. Lett.* **126**, 1–7 doi:10.1016/j.imlet.2009.07.005
3 Carroll, M.C. (1998) The role of complement and complement receptors in induction and regulation of immunity. *Annu. Rev. Immunol.* **16**, 545–568 doi:10.1146/annurev.immunol.16.1.545
4 Ferreira, V.P., Pangburn, M.K. and Cortés, C. (2010) Complement control protein factor H: the good, the bad, and the inadequate. *Mol. Immunol.* **47**, 2187–2197 doi:10.1016/j.molimm.2010.05.007
5 Ricklin, D., Hajishengallis, G., Yang, K. and Lambris, J.D. (2010) Complement: a key system for immune surveillance and homeostasis. *Nat. Immunol.* **11**, 785–797 doi:10.1038/ni.1923
6 Harboe, M. and Mollnes, T.E. (2008) The alternative complement pathway revisited. *J. Cell. Mol. Med.* **12**, 1074–1084 doi:10.1111/j.1582-4934.2008.00350.x
7 Wu, J., Wu, Y.-Q., Ricklin, D., Janssen, B.J.C., Lambris, J.D. and Gros, P. (2009) Structure of complement fragment C3b-factor H and implications for host protection by complement regulators. *Nat. Immunol.* **10**, 728–733 doi:10.1038/ni.1755
8 Kristensen, T. and Tack, B.F. (1986) Murine protein-H ss comprised of 20 repeating units, 61 amino-acids in length. *Proc. Natl. Acad. Sci. U.S.A.* **83**, 3963–3967 doi:10.1073/pnas.83.11.3963
9 Esparza-Gordillo, J., Soria, J.M., Buil, A., Almasy, L., Blangero, J., Fontcuberta, J. et al. (2004) Genetic and environmental factors influencing the human factor H plasma levels. *Immunogenetics* **56**, 77–82 doi:10.1007/s00251-004-0660-7
10 de Córdoba, S.R. and de Jorge, E.G. (2008) Translational mini-review series on complement factor H: genetics and disease associations of human complement factor H. *Clin. Exp. Immunol.* **151**, 1–13 doi:10.1111/j.1365-2249.2007.03552.x
11 Zipfel, P.F., Würzner, R. and Skerka, C. (2007) Complement evasion of pathogens: common strategies are shared by diverse organisms. *Mol. Immunol.* **44**, 3850–3857 doi:10.1016/j.molimm.2007.06.149
12 Schneider, M.C., Prosser, B.E., Caesar, J.J.E., Kugelberg, E., Li, S., Zhang, Q. et al. (2009) *Neisseria meningitidis* recruits factor H using protein mimicry of host carbohydrates. *Nature* **458**, 890–893 doi:10.1038/nature07769
13 Bhattacharjee, A., Oeemig, J.S., Kolodziejczyk, R., Meri, T., Kajander, T., Lehtinen, M.J. et al. (2013) Structural basis for complement evasion by Lyme disease pathogen *Borrelia burgdorferi*. *J. Biol. Chem.* **288**, 18685–18695 doi:10.1074/jbc.M113.459040
14 Sharp, J.A., Echague, C.G., Hair, P.S., Ward, M.D., Nyalwidhe, J.O., Geoghegan, J.A. et al. (2012) *Staphylococcus aureus* surface protein SdrE binds complement regulator factor H as an immune evasion tactic. *PLoS ONE* **7**, e38407 doi:10.1371/journal.pone.0038407
15 Foster, T.J., Geoghegan, J.A., Ganesh, V.K. and Höök, M. (2014) Adhesion, invasion and evasion: the many functions of the surface proteins of *Staphylococcus aureus*. *Nat. Rev. Microbiol.* **12**, 49–62 doi:10.1038/nrmicro3161
16 Ponnuraj, K., Bowden, M.G., Davis, S., Gurusiddappa, S., Moore, D., Choe, D. et al. (2003) A 'dock, lock, and latch' structural model for a staphylococcal adhesin binding to fibrinogen. *Cell* **115**, 217–228 doi:10.1016/S0092-8674(03)00809-2
17 Zhang, X., Wu, M., Zhuo, W., Gu, J., Zhang, S., Ge, J. et al. (2015) Crystal structures of Bbp from *Staphylococcus aureus* reveal the ligand binding mechanism with fibrinogen α. *Protein Cell* **6**, 757–766 doi:10.1007/s13238-015-0205-x
18 Ganesh, V.K., Rivera, J.J., Smeds, E., Ko, Y.-P., Bowden, M.G., Wann, E.R. et al. (2008) A structural model of the *Staphylococcus aureus* ClfA–fibrinogen interaction opens new avenues for the design of anti-staphylococcal therapeutics. *PLoS Pathog.* **4**, e1000226 doi:10.1371/journal.ppat.1000226
19 Xiang, H., Feng, Y., Wang, J., Liu, B., Chen, Y., Liu, L. et al. (2012) Crystal structures reveal the multi-ligand binding mechanism of *Staphylococcus aureus* ClfB. *PLoS Pathog.* **8**, e1002751 doi:10.1371/journal.ppat.1002751
20 Battye, T.G.G., Kontogiannis, L., Johnson, O., Powell, H.R. and Leslie, A.G.W. (2011) *iMOSFLM*: a new graphical interface for diffraction-image processing with *MOSFLM*. *Acta Crystallogr. D Biol. Crystallogr.* **67**, 271–281 doi:10.1107/S0907444910048675
21 Evans, P. (2006) Scaling and assessment of data quality. *Acta Crystallogr. D Biol. Crystallogr.* **62**, 72–82 doi:10.1107/S0907444905036693
22 Collaborative Computational Project, N. (1994) The CCP4 suite: programs for protein crystallography. *Acta Crystallogr. D Biol. Crystallogr.* **50**, 760–763 doi:10.1107/S0907444994003112
23 McCoy, A.J., Grosse-Kunstleve, R.W., Adams, P.D., Winn, M.D., Storoni, L.C. and Read, R.J. (2007) *Phaser* crystallographic software. *J. Appl. Crystallogr.* **40**, 658–674 doi:10.1107/S0021889807021206
24 Murshudov, G.N., Vagin, A.A. and Dodson, E.J. (1997) Refinement of macromolecular structures by the maximum-likelihood method. *Acta Crystallogr. D Biol. Crystallogr.* **53**, 240–255 doi:10.1107/S0907444996012255

25 Emsley, P. and Cowtan, K. (2004) *Coot*: model-building tools for molecular graphics. *Acta Crystallogr. D Biol. Crystallogr.* **60**, 2126–2132 doi:10.1107/S0907444904019158
26 Davis, I.W., Leaver-Fay, A., Chen, V.B., Block, J.N., Kapral, G.J., Wang, X. et al. (2007) Molprobity: all-atom contacts and structure validation for proteins and nucleic acids. *Nucleic Acids Res.* **35**, W375–W383 doi:10.1093/nar/gkm216
27 Jokiranta, T.S., Cheng, Z.-Z., Seeberger, H., Jòzsi, M., Heinen, S., Noris, M. et al. (2005) Binding of complement factor H to endothelial cells is mediated by the carboxy-terminal glycosaminoglycan binding site. *Am. J. Pathol.* **167**, 1173–1181 doi:10.1016/S0002-9440(10)61205-9
28 Jokiranta, T.S., Hellwage, J., Koistinen, V., Zipfel, P.F. and Meri, S. (1998) Each of the three binding sites on factor H interacts with a distinct site on C3b. *Mol. Immunol.* **35**, 360–360 doi:10.1016/S0161-5890(98)90650-2
29 Jòzsi, M., Oppermann, M., Lambris, J.D. and Zipfel, P.F. (2007) The C-terminus of complement factor H is essential for host cell protection. *Mol. Immunol.* **44**, 2697–2706 doi:10.1016/j.molimm.2006.12.001
30 Ferreira, V.P., Herbert, A.P., Hocking, H.G., Barlow, P.N. and Pangburn, M.K. (2006) Critical role of the C-terminal domains of factor H in regulating complement activation at cell surfaces. *J. Immunol.* **177**, 6308–6316 doi:10.4049/jimmunol.177.9.6308
31 Ram, S., Sharma, A.K., Simpson, S.D., Gulati, S., McQuillen, D.P., Pangburn, M.K. et al. (1998) A novel sialic acid binding site on factor H mediates serum resistance of sialylated *Neisseria gonorrhoeae*. *J. Exp. Med.* **187**, 743–752 doi:10.1084/jem.187.5.743
32 Hammerschmidt, S., Agarwal, V., Kunert, A., Haelbich, S., Skerka, C. and Zipfel, P.F. (2007) The host immune regulator factor H interacts via two contact sites with the PspC protein of *Streptococcus pneumoniae* and mediates adhesion to host epithelial cells. *J. Immunol.* **178**, 5848–5858 doi:10.4049/jimmunol.178.9.5848
33 Kajander, T., Lehtinen, M.J., Hyvarinen, S., Bhattacharjee, A., Leung, E., Isenman, D.E. et al. (2011) Dual interaction of factor H with C3d and glycosaminoglycans in host-nonhost discrimination by complement. *Proc. Natl. Acad. Sci. U.S.A.* **108**, 2897–2902 doi:10.1073/pnas.1017087108
34 Pangburn, M.K., Ferreira, V.P. and Cortes, C. (2008) Discrimination between host and pathogens by the complement system. *Vaccine* **26**, I15–I21 doi:10.1016/j.vaccine.2008.11.023
35 Alsenz, J., Lambris, J.D., Schulz, T.F. and Dierich, M.P. (1984) Localization of the complement-component-C3b-binding site and the cofactor activity for factor I in the 38kDa tryptic fragment of factor H. *Biochem. J.* **224**, 389–398 doi:10.1042/bj2240389
36 Schmidt, C.Q., Herbert, A.P., Kavanagh, D., Gandy, C., Fenton, C.J., Blaum, B.S. et al. (2008) A new map of glycosaminoglycan and C3b binding sites on factor H. *J. Immunol.* **181**, 2610–2619 doi:10.4049/jimmunol.181.4.2610
37 Prosser, B.E., Johnson, S., Roversi, P., Herbert, A.P., Blaum, B.S., Tyrrell, J. et al. (2007) Structural basis for complement factor H-linked age-related macular degeneration. *J. Exp. Med.* **204**, 2277–2283 doi:10.1084/jem.20071069
38 Blaum, B.S., Hannan, J.P., Herbert, A.P., Kavanagh, D., Uhrin, D. and Stehle, T. (2015) Structural basis for sialic acid–mediated self-recognition by complement factor H. *Nat. Chem. Biol.* **11**, 77–82 doi:10.1038/nchembio.1696
39 Morgan, H.P., Schmidt, C.Q., Guariento, M., Blaum, B.S., Gillespie, D., Herbert, A.P. et al. (2011) Structural basis for engagement by complement factor H of C3b on a self surface. *Nat. Struct. Mol. Biol.* **18**, 463–470 doi:10.1038/nsmb.2018
40 Hair, P.S., Echague, C.G., Sholl, A.M., Watkins, J.A., Geoghegan, J.A., Foster, T.J. et al. (2010) Clumping factor A interaction with complement factor I increases C3b cleavage on the bacterial surface of *Staphylococcus aureus* and decreases complement-mediated phagocytosis. *Infect. Immun.* **78**, 1717–1727 doi:10.1128/IAI.01065-09
41 Dunkelberger, J.R. and Song, W.-C. (2010) Complement and its role in innate and adaptive immune responses. *Cell Res.* **20**, 34–50 doi:10.1038/cr.2009.139

